Quantitative understanding of HepaRG cells during drug-induced intrahepatic cholestasis through changes in bile canaliculi dynamics

Sonoi, Rie
Biomedical Research Institute, National Institute of Advanced Industrial Science and Technology

Hagihara, Yoshihisa
Biomedical Research Institute, National Institute of Advanced Industrial Science and Technology

出版情報：Pharmacology Research and Perspectives (PRP). 10 (3), pp.e00960-, 2022-05-27. American Society for Pharmacology and Experimental Therapeutics (ASPET)
バージョン：

Received: 22 February 2022 | Accepted: 18 April 2022

DOI: 10.1002/prp2.960

ORIGINAL ARTICLE

Quantitative understanding of HepaRG cells during drug-induced intrahepatic cholestasis through changes in bile canaliculi dynamics

Rie Sonoi | **Yoshihisa Hagihara**

Biomedical Research Institute, National Institute of Advanced Industrial Science and Technology, Ikeda, Osaka, Japan

Correspondence
Rie Sonoi, Biomedical Research Institute, National Institute of Advanced Industrial Science and Technology, 1-8-31 Midorigaoka, Ikeda, Osaka 563-8577, Japan.
Email: sonoi-r@staff.kanazawa-u.ac.jp

Present address
Rie Sonoi, Nano Life Science Institute, Kanazawa University, Kakuma-machi, Kanazawa, Ishikawa 920-1164, Japan

Funding information
Japan Agency for Medical Research and Development, Grant/Award Number: 19be0304101h0003

Abstract

An understanding of the quantitative relationship between bile canaliculus (BC) dynamics and the disruption of tight junctions (TJs) during drug-induced intrahepatic cholestasis may lead to new strategies aimed at drug development and toxicity testing. To investigate the relationship between BC dynamics and TJ disruption, we retrospectively analyzed the extent of TJ disruption in response to changes in the dynamics of BCs cultured with entacapone (ENT). Three hours after adding ENT, the ZO-1-negative BC surface area ratio became significantly higher (4.1-fold) than those of ZO-1-positive BCs. Based on these data, we calculated slopes of surface area changes, m, of each ZO-1-positive and ZO-1-negative BC. BCs with $m \leq 15$ that fell within the 95% confidence interval of ZO-1-positive BCs were defined as ZO-1-positive. To validate this method, we compared the frequency of ZO-1-positive BCs, F_Z, with that of BCs with $m \leq 15$, F_T, in culture using drugs that regulate TJ, or induce intrahepatic cholestasis. F_T values were correlated with F_Z under all culture conditions ($R^2 = .99$). Our results indicate that the magnitude of BC surface area changes is a factor affecting TJ disruption, suggesting that maintaining TJ integrity by slowing BC dilation inhibits cell death.

KEYWORDS
bile canaliculus, bile canaliculus dynamics, drug-induced intrahepatic cholestasis, non-invasive evaluation, tight junction, zonula occludens-1

1 | INTRODUCTION

Drug-induced liver injuries lead to serious adverse events. As such, it is necessary to evaluate the possibility that a new drug may induce intrahepatic cholestasis, prior to human clinical trials. However, using data gathered from animal experiments to accurately predict drug cytotoxicity in humans is difficult due to differences between the drug related metabolic processes in humans and rodents.[1,2] By contrast, using an alternative method, such as that based on a human-cell-based-assay via organ(s)-on-a-chip, may provide important information regarding the effect and safety of new drugs. Moreover, human HepaRG cells, which provide reproducible data, present an attractive cell source that exhibit the same functional structure as that of mature hepatocytes, as well as correctly polarized distributions

Abbreviations: BC, bile canaliculus; ENT, entacapone; FOR, forskolin; TJs, tight junctions; TOL, tolcapone; ZO-1, zonula occludens-1.

of transport proteins.[3] Research studies aimed at developing tools required for this assay are currently in progress[4–6]; hence, a suitable quantitative evaluation method is needed. In particular, the establishment of quantitative evaluation methods that reflect changes in cell characteristics would enable large amounts of data involved in drug screening to be accurately and easily evaluated, leading to the development of new technologies that can be utilized to regulate cell characteristics and dynamics via established parameters.

Drugs that cause intrahepatic cholestasis are known to inhibit hepatic transporter functions, resulting in hepatotoxicity due to the accumulation of bile acids in the cytosol or in the bile canaliculi (BCs) of hepatocytes.[7,8] Meanwhile, the Rho small GTPase family regulates the assembly and disassembly of the actin cytoskeleton,[9] and drugs that induce intrahepatic cholestasis have been found to alter BC dynamics via the Rho kinase/myosin light kinase pathway.[10,11] The actin cytoskeleton and adapter proteins, such as zonula occludens-1 (ZO-1), interact to form tight junctions (TJs),[12,13] while certain drugs may cause the interaction between TJs and the actin cytoskeleton to become unbalanced, thereby disrupting TJ integrity.[14] Thus, an investigation of BC dynamics may provide important information regarding changes in cellular fate.

Clinical trial data has revealed that tolcapone (TOL) and entacapone (ENT), which are clinically used to treat patients with Parkinson's syndrome, evoke intrahepatic cholestasis.[15,16] More specifically, exposure to TOL and ENT causes BC dilation via the Rho kinase/myosin light kinase pathway.[10,11] A previous retrospective study analyzed time-lapse and immunofluorescence images of the TJ protein, ZO-1, in BCs cultured with or without ENT and forskolin (FOR), a drug that facilitates TJ formation, to better understand the effects of TJ structural changes due to altered BC dynamics.[14] Moreover, we previously found that exposure to ENT and FOR suppresses changes in BC dynamics, resulting in inhibition of TJ disruption and apoptosis. Taken together, these findings indicate that rapidly changing BC dynamics may be a key factor in changing cell fate toward death during drug-induced intrahepatic cholestasis.

In the present study, we aimed to establish a non-invasive and quantitative evaluation method based on changes in the size of BCs in HepaRG cells during drug-induced intrahepatic cholestasis. To this end, we conducted a retrospectively investigated the relationship between BC size and TJ disruption in HepaRG cells exposed to TOL or ENT.

2 | MATERIALS AND METHODS

2.1 | Culture conditions of HepaRG cells

Cryopreserved, differentiated HepaRG cells (Lot. No. HPR116293-TA08; Biopedric International) were seeded at a density of 2.1×10^5 cells/cm^2 in 6-well plates (Corning) and maintained for 14 days at 37°C in a humidified 5% CO_2 incubator. The maintenance medium, which was prepared according to the supplier's instructions (Biopedric International), was changed every 2 days. After 14 days, mature HepaRG cells, with TJs sealing canalicular lumen to form BCs, were incubated for 48 h in culture medium containing 1.7% dimethyl sulfoxide (DMSO) with, or without, ENT (100 μM; Sigma-Aldrich), TOL (100 μM; Tokyo Chemical Industry Corporation), or FOR (10 μM; FUJIFILM Wako Pure Chemical Corporation) at 37°C in a humidified 5% CO_2 environment. Exposure time, *t*, was determined from the moment following the addition of ENT, TOL, or FOR. To understand the changes in BC dynamics following exposure to drugs, the exposure time and concentration of drugs were determined based on the cytotoxicity data and BC dynamics in published reports.[10,14]

2.2 | Time-lapse monitoring and immunofluorescence staining

Time-lapse images of HepaRG cells were captured from triplicate cultures in 6-well plates using an image analyzer (Eclipse Ti2; Nikon) with a 10× objective lens and phase-contrast images (5.3 × 5.3 mm) at 16 bits in gray scale with 1.88 pixels/μm^2 resolution, every 20 min for 48 h. Following time-lapse observation, fluorescence staining of ZO-1 protein (Abcam), F-actin, and cell nuclei of HepaRG cells was conducted according to a previously described method.[14] Briefly, HepaRG cells washed with PBS were fixed with 2% paraformaldehyde for 15 min at 4°C, and permeabilized by incubation for 30 min in 0.05% Triton X-100 at 4°C. Nonspecific binding of antibodies was blocked by treatment with Block Ace (Dainippon Sumitomo Pharma) overnight at 4°C. The cells were incubated with primary antibodies (1:200 dilution) overnight at 4°C. After washing with PBS, HepaRG cells were incubated with Alexa Fluor 488-conjugated goat anti-rabbit IgG (Abcam), 4',6-diamidino-2-phenylindole (DAPI, Life Technologies Corporation), and Alexa Fluor 594 phalloidin (Invitrogen) for 3 h at 26±2°C. Fluorescence images were captured using a fluorescence microscope with a 10× objective lens (Eclipse Ti2; Nikon). Fluorescence signal intensities were obtained via excitation at corresponding wavelengths of 358, 488, and 594 nm.

2.3 | Quantitative analyses of bile canaliculus surface areas and the extent of tight junction disruption

A schematic outline of the data analysis procedure for the BC surface area and extent of TJ disruption is shown (Figure 1). To measure the surface areas of BCs in the regions of interest (ROIs), 300 ×300 μm ROIs were randomly selected from three measurement regions in a culture vessel, via three independent experiments. Data were obtained from nine ROIs under each culture condition (3 ROIs in a culture dish ×3 independent experiments). To analyze the time-dependent changes occurring in BC dynamics, a surface area of each individual BC, *A*, from phase-contrast image datasets was manually measured using ImageJ software,[17] every 1 h for 48 h. The surface areas of BCs in a culture condition with ENT, A_{ENT}, or without ENT, A_{Ctrl}, were calculated. The A_{ENT} and A_{Ctrl} values were used to estimate the index of BC dilation, defined as the ratio between the surface areas of BCs

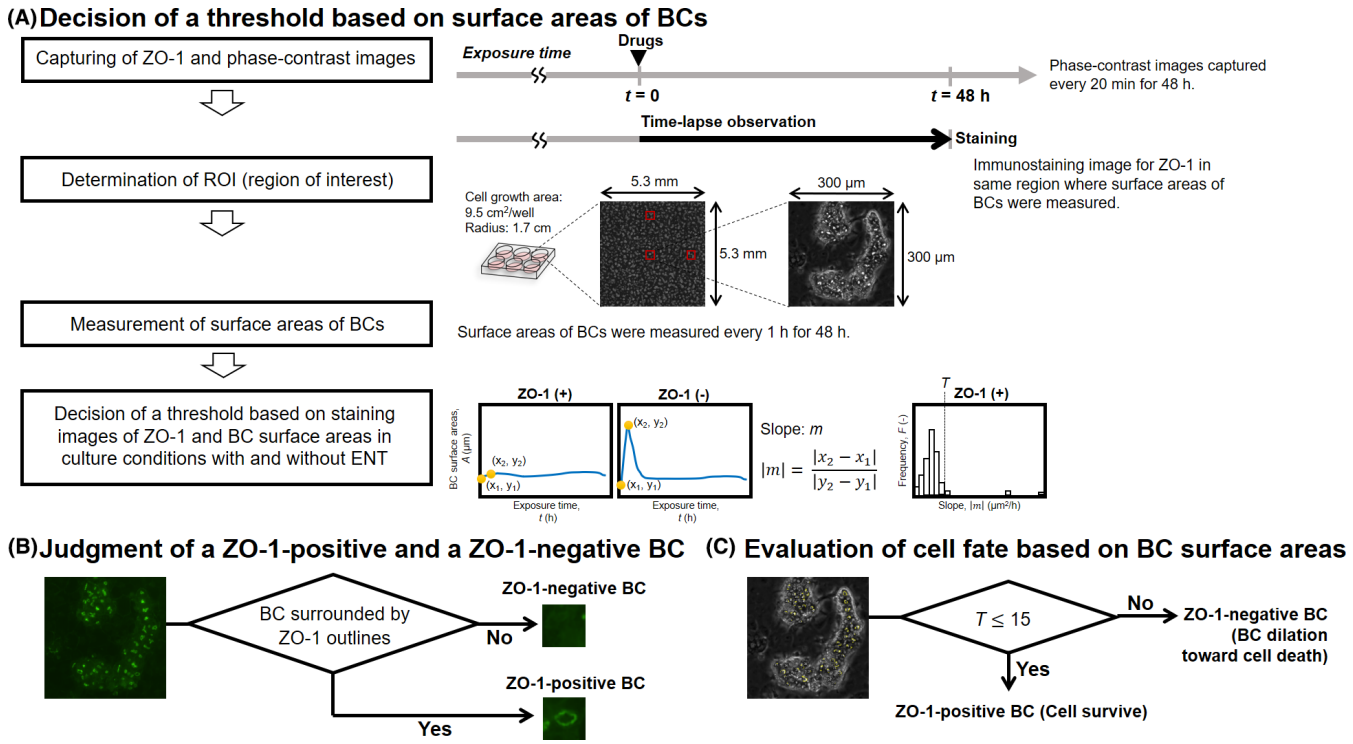

FIGURE 1 Data analysis procedure pertaining to changes in BC surface areas in HepaRG cells during drug-induced intrahepatic cholestasis. A schematic outline shows decision of a threshold based on surface areas of BCs (A), Judgment of a ZO-1-positive and a ZO-1-negative BC (B), and evaluation of cell fate based on BC surface areas.

cultured with ENT and the average values of the surface area for all BCs cultured without ENT, $A_{ENT}/\overline{A_{Ctrl}}$, in each ROI, every 1 h for 48 h.

To confirm and quantify the association between BC surface area and the extent of TJ disruption, ZO-1 immunostaining images were captured following time-lapse monitoring of the same positions where BC surface area had been measured. Fluorescence stained images of F-actin and cell nuclei were used as reference data to understand the cellular structure of HepaRG cells under all culture conditions. The BCs of HepaRG cells were divided into ZO-1-positive and ZO-1-negative groups, according to the criteria depicted in Figure 1. ZO-1-positive and ZO-1-negative BCs were retrospectively identified and their respective frequencies, F_Z and F_N, were estimated, respectively. To compare the magnitude of changes between the surface areas of individual ZO-1-positive and ZO-1-negative BCs, the surface area ratio for individual BCs, R_A, was calculated using the surface area of each ZO-1-positive or ZO-1-negative BC and the $\overline{A_{Ctrl}}$ value. The slope, m, of BC surface areas versus exposure times from $t = 0$ to 3 h, was calculated, and the threshold, T, which distinguishes ZO-1-positive BC (cell survival) or ZO-1-negative BC (BC dilation toward cell death) was determined. These slopes were estimated using the data obtained from HepaRG cells cultured with or without ENT, following which, the average values of the slopes for ZO-1-positive and ZO-1-negative BCs were calculated. T was defined as the value that was two standard deviations away from the mean of the surface areas of ZO-1-positive BCs cultured with, or without, ENT. Data were obtained from 10–50 BCs in the ROI from $t = 0$ to 48 h, with the ROIs selected from three independent experiments.

To ascertain the established evaluation index, the frequency of ZO-1-positive BCs, F_Z, and the frequency of BCs with a value less than that of T, F_T, was calculated using the data from the BCs in ROIs under each culture condition, respectively, following which F_Z and F_T values were compared. Our established evaluation method was validated using data from HepaRG cells cultured without drugs, and those cultured with TOL, FOR, TOL/FOR, and ENT/FOR, respectively.

2.4 | Statistical analysis

Data were expressed as mean ± standard deviation, and comparisons between the groups were analyzed using one-way analysis of variance (ANOVA) followed by the Tukey–Kramer post-hoc test. The Student's t-test was used to determine statistically significant differences between two samples. Statistical significance was set at $^{*}p < .05$ and $^{**}p < .01$.

3 | RESULTS

3.1 | Tight junction disruption as a consequence of drastic changes in bile canaliculus dynamics

Time-lapse monitoring and ZO-1 immunofluorescence staining were conducted for HepaRG cells cultured with, or without ENT (100 μM), at $t = 0$–48 h (Video S1). At $t = 0$, BCs were formed between HepaRG cells

under both culture conditions. HepaRG cells cultured with ENT exhibited rapid dilation of BCs during $t = 0$–3 h. As cell culture proceeded, the BCs in HepaRG cells cultured with ENT gradually became smaller, and finally disrupted. Ultimately, the constricted BCs in HepaRG cells cultured with ENT detached from the culture vessel. However, such drastic changes were not observed in the dynamics of BCs in HepaRG cells cultured without ENT. Under both culture conditions, cells exhibiting minute alterations in the size of BCs were surrounded by a distinct line of ZO-1. Conversely, cells exhibiting drastic alterations in the size of BCs did not express ZO-1 around BCs (Video S1).

To quantitatively analyze TJ disruption in response to changes in BC dynamics, a time profile of the surface areas of ZO-1-positive and ZO-1-negative BCs in HepaRG cells cultured with, or without, ENT was constructed. The ratio of surface areas of BCs cultured with ENT *vs* those without ENT, $A_{ENT}/\overline{A_{Ctrl}}$, was estimated based on the data of BC surface areas under both culture conditions in triplicate experiments (Figure 2). The $A_{ENT}/\overline{A_{Ctrl}}$ of ZO-1-positive BCs (0.6 ± 0.15) was the same as the $A_{ENT}/\overline{A_{Ctrl}}$ of ZO-1-negative BCs (1.0 ± 0.25) (Figure 2). As exposure time elapsed, the value of $A_{ENT}/\overline{A_{Ctrl}}$ of ZO-1-negative BCs increased rapidly to 3.9 ± 0.46 at $t = 3$ h, with the slope of ZO-1-negative BCs becoming steeper at $t = 0$–3 h. Until $t = 48$ h, the value of $A_{ENT}/\overline{A_{Ctrl}}$ of ZO-1-negative BCs decreased gradually to 1.7 ± 0.31. In ZO-1-positive BCs, the values of $A_{ENT}/\overline{A_{Ctrl}}$ remained at 1 from $t = 0$ to 48 h.

3.2 | Correlation between tight junction disruption and bile canaliculus dynamics changes

Frequencies of ZO-1-positive, F_Z, or ZO-1-negative, F_N, BCs under both culture conditions were compared in relation to BC size and the extent of TJ disruption. Between $t = 0$ and 6 h, the distribution of A of ZO-1-positive BCs ranged from 0 to 2.8 (Figure 3) and exhibited a Gaussian distribution pattern. There was no change in the distribution of A of ZO-1-positive BCs until $t = 48$ h (Figure 3). Meanwhile, the distributions of A of ZO-1-negative BCs from $t = 0$ to 12 h were broader, ranging from 0 to 12, while that of A of ZO-1-negative BCs from $t = 42$ to 48 h was narrower than that from $t = 0$ to 12 h (Figure 3).

To classify non-invasive ZO-1-positive and ZO-1-negative BCs, we focused on the slopes of the surface area plots for individual ZO-1-positive BCs, m, from $t = 0$ to 3 h, based on a large difference in the slopes of time-dependent increases in the average surface area values for individual ZO-1-positive and ZO-1-negative BCs (Figure 2). BCs under both culture conditions were divided into ZO-1-positive, and a ZO-1-negative BC groups, based on the standard deviations and mean of absolute values of the surface area slopes for ZO-1-positive BCs. A threshold based on the slopes of the surface area plots for individual ZO-1-positive BCs under both culture conditions, T, was defined as the value that two standard deviations away from the average absolute value of the slopes of the surface area plots for individual ZO-1-positive BCs from $t = 0$ to 3 h (Figure S1).

The extent of TJ disruption, frequencies of ZO-1-positive BCs, F_Z, and BCs less than T, F_T, were investigated to compare the changes in BC size in cells cultured with, or without, ENT. The frequency of ZO-1-positive BCs in cultures without ENT was over 3.0-fold higher than that in cultures with ENT ($F_Z = 0.98 \pm 0.03$ and $F_Z = 0.33 \pm 0.13$, respectively; Figure 4). The F_T value (0.97 ± 0.03) of cells cultured with ENT differed significantly compared to that (0.42 ± 0.18) of cells cultured without ENT. The F_T values as well as F_Z values of BCs of ENT-exposed HepaRG cells were significantly lower than those of BCs unexposed to ENT, indicating that exposure to ENT led to the disruption of TJs (Figure 4). There was high concordance between the F_Z and F_T of those cultured with or without ENT (99% and 78%, respectively).

3.3 | Slow dilation of bile canaliculus prevents tight junction and bile canaliculus disruption

The association between TJ disruption and BC dynamics in HepaRG cells cultured with FOR, ENT, TOL, TOL/FOR, and ENT/

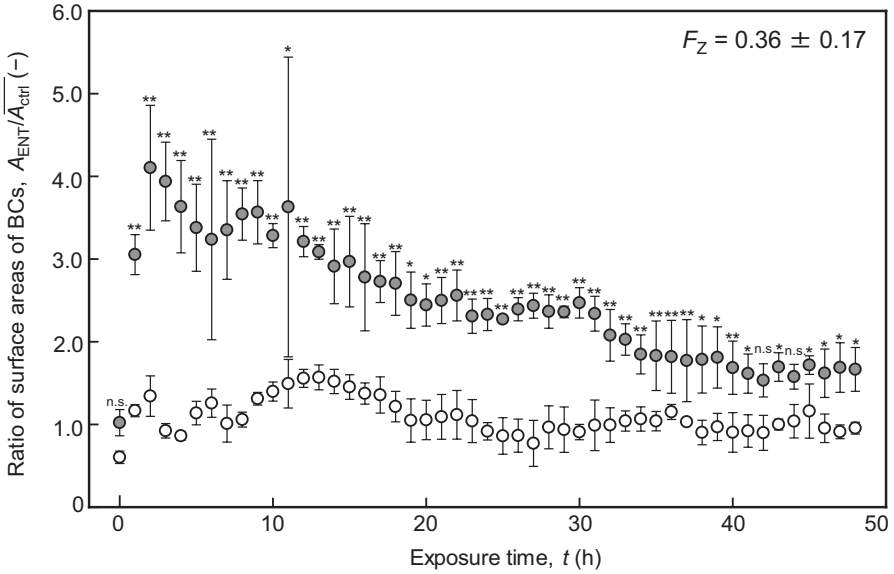

FIGURE 2 Time course of surface areas of BCs of HepaRG cells cultured with, or without, ENT. Open circles, ZO-1-positive BCs; shaded circles, ZO-1-negative BCs. Data were obtained from three independent cultures. The data were obtained from BCs that can be traced continuously in the ROI at $t = 0$–48 h. Statistical significance for Student's t-test was set at $^*p < .05$; or $^{**}p < .01$.

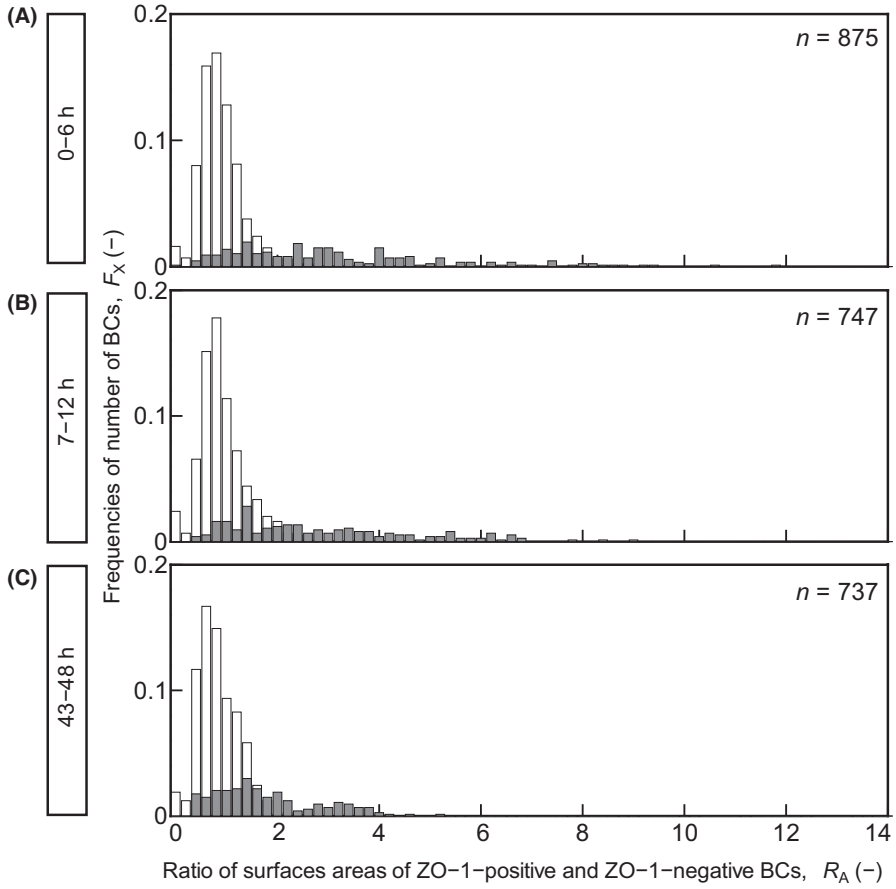

FIGURE 3 Frequencies of ZO-1-positive and ZO-1-negative BCs of HepaRG cells cultured with, or without ENT. Open bars, ZO-1-positive BCs; shaded bars, ZO-1-negative BCs. R_A, which is defined as a ratio of surface areas of individual BCs, was calculated from each surface area of ZO-1-positive or ZO-1-negative BCs and the $\overline{A_{Ctrl}}$ value. Data were obtained from 700–900 BCs in ROIs in both culture conditions at t = 0–6 h, (A), t = 7–12 h (B), and t = 43–48 h (C). The judgment of a ZO-1-positive and a ZO-1-negative BC was determined using immunostaining image for ZO-1 in the same region where areas of BCs were measured.

FOR, or without drugs, was studied from t = 0 to 48 h, via time-lapse monitoring and ZO-1 immunofluorescence staining (Videos S2–S4). FOR was used to facilitate TJ formation in HepaRG cells that had reached the stage of maturity ideal for TJ formation, however, no change was observed in BC dynamics or TJ formation (Video S2). The BCs in HepaRG cells cultured with ENT or TOL dilated rapidly from t = 0 to 3 h. However, as exposure time elapsed, the dilation of BCs reached a limit, following which some cells detached from the surface of the culture dish (Videos S3 and S4). Meanwhile, simultaneously adding FOR with either ENT or TOL to HepaRG cells, caused the BCs to dilate slowly, as a result of which the BC network remained intact until t = 48 h (Videos S3 and S4). Under all culture conditions, BCs exhibiting slow dilation were ZO-1-positive, while BCs showing rapid dilation were ZO-1-negative (Videos S2–S4).

To ascertain the effect of BC dilation on the TJs of HepaRG cells during the early phase of drug-induced intrahepatic cholestasis, the slopes of the surface area plots for the BCs, m, of HepaRG cells cultured without drugs, as well as those cultured with ENT, FOR, TOL, TOL/FOR, or ENT/FOR were investigated from t = 0 to 3 h. The m values of HepaRG cells cultured without drugs and with FOR were 4.9 ± 0.92 and 6.0 ± 0.89, respectively (Figure 5). When exposed to ENT or TOL, the m values of drug-exposed HepaRG cells were significantly higher than those of unexposed HepaRG cells (7.7-fold or 14-fold, respectively). Meanwhile, the m values of ENT/FOR- or TOL/FOR-exposed HepaRG cells were 18 ± 3.3 and 18 ± 3.7, respectively, and were significantly reduced when compared with those of ENT- or TOL-exposed HepaRG cells.

To validate the evaluation method based on T, we compared the frequencies of ZO-1-positive BCs, F_Z, and frequencies of the number of BCs with values less than T, F_T, of HepaRG cells cultured without drugs, as well as of those cultured with FOR, ENT, TOL, TOL/FOR, or ENT/FOR from t = 0 to 48 h. Under all culture conditions, the values of F_Z and F_T were closely correlated (R^2 = .99); (Figure 6). The F_Z and F_T values of ENT/FOR- or TOL/FOR-exposed HepaRG cells were significantly higher than those of ENT- or TOL-exposed HepaRG cells (Figure 6), indicating that exposure to FOR suppressed TJ disruption and the change in BC dynamics in HepaRG cells cultured with TOL or ENT.

4 | DISCUSSION

4.1 | Changes in bile canaliculus dynamics and tight junction disruption

The present study quantitatively demonstrated that slowing BC dilation prevents TJ disruption. Although the mechanisms underlying drug-induced intrahepatic cholestasis have not been well defined, alterations in hepatobiliary transporters, changes in cell polarity,

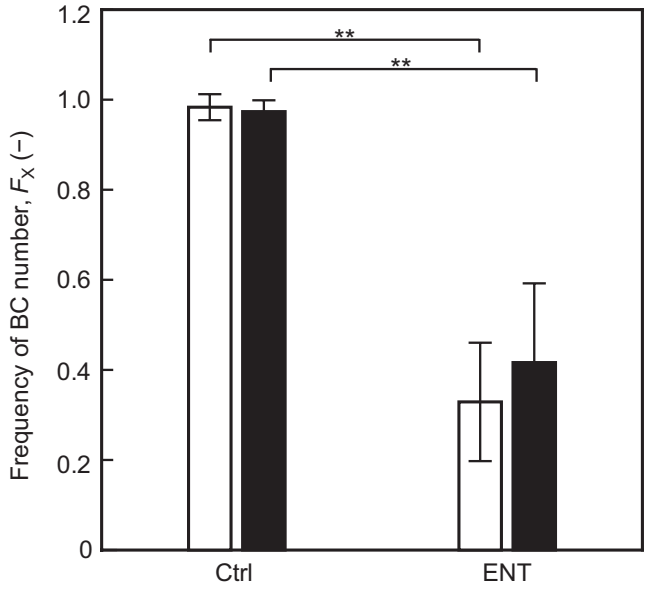

FIGURE 4 Comparison between the frequencies of ZO-1-positive BCs and BCs less than *T*, cultured with or without ENT. Open bars, frequency of number of ZO-1-positive BCs, F_Z; Closed bars, frequency of number of BCs having less than the *T* value, F_T. Data were obtained from three independent experiments. Statistical significance was determined via one-way analysis of variance (ANOVA) followed by Tukey-Kramer post-hoc test (**$p < .01$).

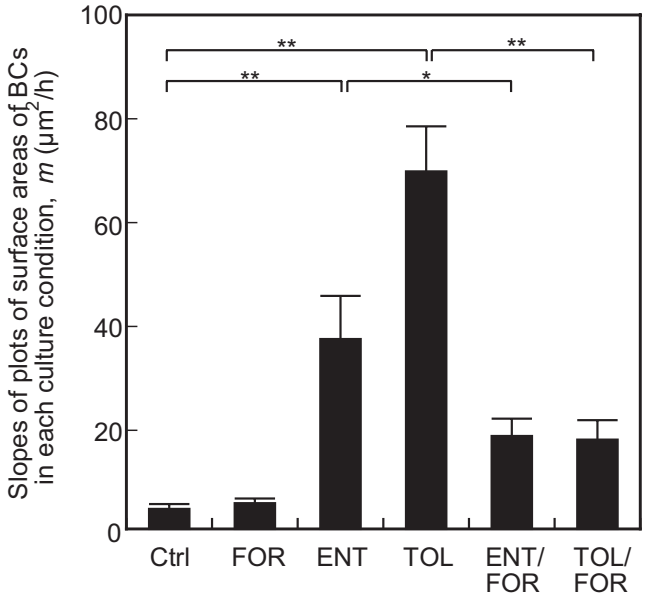

FIGURE 5 Effect of BC dynamics changes on TJ formation Closed bars, slopes of plots of surface areas of BCs, *m*, of HepaRG cells in each culture without drugs (Ctrl), those cultured with FOR, with ENT, with TOL, with TOL/FOR, and with ENT/FOR at $t = 0$–48 h. Data were obtained from three independent experiments. Statistical significance was determined via one-way analysis of variance (ANOVA) followed by Tukey-Kramer post-hoc test (**$p < .01$; * $p < .05$).

disruption of cell-cell junctions, and changes in the cytoskeleton are thought to participate in the development of intrahepatic cholestasis. Thus, the present study focused on the BC dynamics that are essential for bile acid flux as predictive nonclinical markers of drug-induced cholestasis. More specifically, we attempted to quantitatively analyze the association between BC dynamics and the extent of TJ disruption, by evaluating the correlation between the changes that occur in BC surface area and the extent of TJ disruption. We quantitatively established that changes in BC surface area corresponding to *m* values ≤15, during the early phase of drug-induced intrahepatic cholestasis process, did not lead to cell death via TJ disruption. Bile acids, which regulate hepatocyte polarization and canalicular formation,[18,19] are synthesized from cholesterol in hepatocytes and secreted by transporters, such as the bile salt export pump (BSEP), into the BC. Thus, drug-induced impairment of BC dynamics or transporter inhibition cause bile secretory failure, suggesting that maintenance of polarization is essential for hepatocyte function. Meanwhile, exposure of HepaRG cells to TOL causes inhibition of BSEP, whereas exposure to ENT does not inhibit BSEP or other transporters.[10] Nevertheless, both TOL and ENT induce impairment of BC dynamics,[10] which was confirmed by the results of the current study (Videos S1 and S4). Burbank et al.[10] reported the presence of early BC deformities in contraction or dilation of the BC associated with changes in the ROCK/MLCK pathway following treatment with all tested drugs, including those that were not BSEP inhibitors. Hence, early changes in BC dynamics associated with the ROCK/MLCK pathway may serve as specific predictive markers that can provide information regarding the cholestatic potential of novel drugs.

The TJ scaffolding protein, ZO-1, is linked to actin-biding sites, where actin assembly and disassembly are regulated by Rho family small GTPases.[12,13,20,21] Exposure of cells to TOL and ENT, which are known to induce hepatic cholestasis, accelerates BC dilation by relaxing actomyosin via the Rho kinase/myosin light kinase pathway.[10,11] Rapid BC dilation causes BC disruption, resulting in TJ disruption and apoptosis.[14] Meanwhile, exposing HepaRG cells cultured with ENT or TOL to FOR suppressed BC dilation (Figures 5 and 6), and maintained TJ integrity in BCs. Interestingly, despite the strong mitochondrial toxicity of TOL,[22,23] adding FOR to TOL slowed the expansion of BC surface areas and localization of ZO-1 on the membrane of BCs. It has been previously reported that FOR promotes BC network formation in hepatocytes by activating cAMP and promoting TJ formation.[18] Gao et al.,[24] reported that FOR reinforces the integrity of cell-cell contacts in renal glomerular epithelial cells, namely podocytes, via Rho family small GTPases signaling, resulting in the closure of an intercellular adhesion zipper, accompanied by redistribution of cell adhesion molecules and actin-associated proteins in a continuous linear pattern at cell-cell contact points. The results of the current study suggest that FOR, which activates cAMP and modulates the Rho-GTPase-dependent actin cytoskeleton, enhances BC structure and suppresses BC disruption, thereby facilitating TJ formation and suppressing cell death.

In the present study, ZO-1 was selected as an invasive indicator of the correlation between BC dynamics and TJ disruption as ZO-1 is

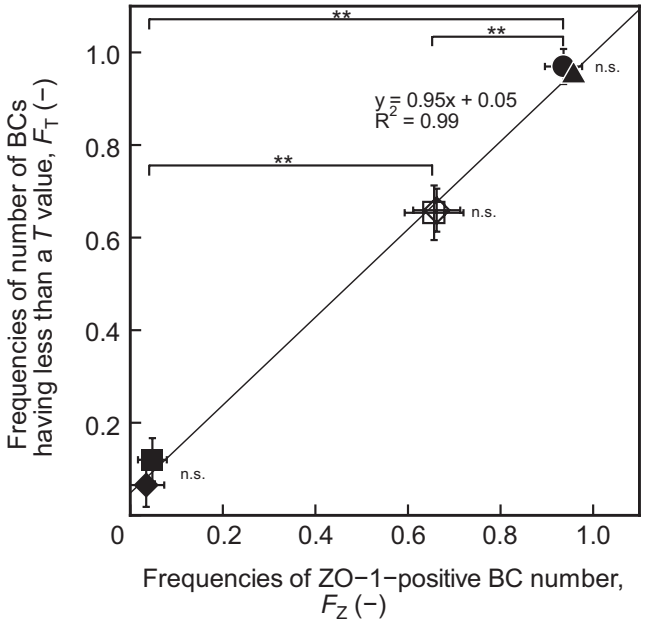

FIGURE 6 Correlation between F_Z and F_T values of HepaRG cells cultured without drugs, and those cultured with FOR, ENT, TOL, TOL/FOR, or ENT/FOR from $t = 0$–48 h. Closed circles, without drugs; Closed triangles, with FOR; Closed squares, with ENT; Closed rhombuses, with TOL; Open squares, with ENT/FOR; Open rhombuses, with TOL/FOR. Data were obtained from three independent experiments. Statistical significance was determined via one-way analysis of variance (ANOVA) followed by Tukey-Kramer post-hoc test (**$p < .01$). Pearson correlation coefficients were used to evaluate the relationship between F_Z and F_T values, and the equation were calculated using least-squares analysis.

able to change its subcellular localization in rearrangements to perturb the uniform, continuous localization of TJ proteins along cell-cell junctions, thus disrupting barrier function. This report supports our strategy of analyzing TJ disruption based on the categorization of individual BCs as either ZO-1-positive BCs with a perfectly distinct line of ZO-1 surrounding BCs, or as ZO-1-negative BCs with an imperfect line of ZO-1 surrounding BCs. In a previous study, we reported that culturing with Y27632 (i.e., ROCK inhibitor) induces BC disruption in HepaRG aggregates, while upregulation of cell growth results in the reformation of BCs.[25] In a previous study, regulation of cell proliferation via the nuclear translocation of ZO-1 from the cellular membrane of BCs following TJ disruption was considered to be related to the reformation of BCs.,[25] ZO-1 is a regulator of contact inhibition[26,27] and is sensitive to mechanical stimulation, causing it to alter its subcellular localization.[28,29] Schwayer et al.[30] reported that accumulation of ZO-1 in the TJs of zebrafish embryos is closely associated with tension in the adjacent actomyosin network as these junctions are mechanosensitive. These reports indicate that mechanical interactions between actin TJs are important for maintaining hepatocyte polarity and function. In the present study, $A_{ENT}/\overline{A_{Ctrl}}$ values of ZO-1-positive BCs were higher than those of ZO-1-negative BCs, indicating that the magnitude of BC dynamics, that was changed via actin dynamics, was associated with TJ disruption in BCs (Figure 2). Exposure to FOR facilitated TJ formation, causing a significant decrease in the *m* values of HepaRG cells cultured with ENT or TOL (Figure 5). Moreover, correlation analysis revealed that the F_Z values showed a high level of association with F_T values (Figure 6). These findings indicate that BC dynamics and ZO-1 are important indicators of changes in cellular properties during drug-induced intrahepatic cholestasis.

4.2 | Non-invasive evaluation based on bile canaliculi dynamics changes

Long-term time-lapse monitoring is affected by focus drift. Further, temperature changes can affect focus drift and, as such, must be taken into consideration. However, microscopes that reduce focus drift[31–33] require customized optical components and hardware making them very costly. Although techniques, such as image processing via deep learning,[34] may be used to solve out-of-focus blurring, we established an evaluation method that simplifies data processing and allows it to be easily analyzed. The proposed analytical method, which is based on a plot of two points where the slope of the surface area of a BC is maximum, allows information to be obtained in a short time with a small number of images.

A retrospective analysis using time-lapse and ZO-1 staining images was performed to establish a method for evaluating BC dynamics in drug-induced hepatic cholestasis. Our analysis revealed that drastic changes that took place during the early phase of BC dilation were essential to TJ disruption. This analytical method has been used to investigate the association between changes in the behavior, morphology and characteristics of cells[35,36] to retrospectively ascertain the "factors" that led to the "result" in each process. Therefore, we evaluated the relationship between the extent of TJ disruption and BC dynamics and found that rapid changes taking place in BCs during the early phase of drug-induced intrahepatic cholestasis process (slope of a line of plots of BC surface area >15) lead to TJ disruption. Interestingly, when exposed to ENT and FOR simultaneously, BCs turned ZO-1 positive despite expanding (Figure 5). This may be due to the simultaneous exposure to ENT and FOR slowing BC dilation, thus allowing them to maintain their structure and facilitating TJ formation. Based on our retrospective analysis, it is proposed that changes in the size of BCs during the early phase of BC dynamics, as represented by *m*, is a factor that affects BC structure as well as cell death.

Evaluating changes in BC surface area during the early stages of the drug-induced intrahepatic cholestasis, led to a better understanding of the non-invasive potential of ZO-1-positive and ZO-1-negative BCs. The F_T value, an evaluation index based on the slope of the BC surface area plot in cultures exposed, or unexposed, to ENT, was compared with the frequency of ZO-1 positive BCs, F_Z. The results showed high agreement (99%) between F_Z and F_T values under culture conditions without ENT. This indicates that the ratio of changes in BC surface areas allowed non-invasive discrimination between ZO-1-positive and ZO-1-negative BCs at $t = 48$ h. Interestingly, under culture conditions with ENT and FOR, as well

as with TOL and FOR, BCs turned ZO-1 positive as a consequence of the dilation caused by ENT or TOL, being slowed down. These results indicate that slow dilation of BC is critical for maintaining BC structure. That is, the evaluation index, which distinguishes ZO-1-positive from ZO-1-negative BCs, is not the integrated value but the derivative value. It is suggested that the differential value, which indicates the amount of instantaneous change, that is, the rate of change in BC size during the early phase of BC dilation, is an important parameter that governs BC structural changes. Considered together, we propose that a non-invasive evaluation method would help better understand TJ disruption as a consequence of changes in BC dynamics during drug-induced intrahepatic cholestasis.

5 | CONCLUSION

Our retrospective analysis revealed that ZO-1-negative BCs exhibiting TJ disruption show steeper slopes in BC surface areas for 3 h following the addition of ENT or TOL. Conversely, no significant differences were observed between the slopes of the surface areas of ZO-1-positive BCs. To differentiate between ZO-1-negative and ZO-1-positive BCs, the slopes, m, of surface area plots for individual ZO-1-positive BCs were estimated 3 h after the addition of ENT. Frequencies of ZO-1-positive BCs were in high agreement with the frequencies of the number of BCs showing $m \leq 15$. Meanwhile, exposure to FOR facilitated TJ formation. Frequencies of the number of BCs with $m \leq 15$ in ENT/FOR- or TOL/FOR-exposed HepaRG cells were significantly higher than those in ENT- or TOL-exposed HepaRG cells. Interestingly, under all culture conditions, the frequency of ZO-1-positive BCs and the frequency of BCs with $m \leq 15$ were closely correlated. Thus, the findings of the present study demonstrate that changes in BC dynamics should be considered as important factors when evaluating TJ disruption and cell death during drug-induced intrahepatic cholestasis. As such, these findings inform the development of therapies and toxicity assessment methods for drug-induced intrahepatic cholestasis.

AUTHOR CONTRIBUTION

RS conceived the study and designed the experiments. RS and YH performed the experiments and interpreted the data. RS and YH wrote the manuscript. Both authors have read and revised the manuscript.

ETHICAL APPROVAL

I declare that this paper follows the policies of pharmacology research & perspectives as outlined in the Ethical Statement.

ACKNOWLEDGMENTS

This research was supported by Japan Agency for Medical Research and Development (AMED) under Grant Number 19be0304101h0003.

DISCLOSURE

The authors declare that they have no competing interests.

DATA AVAILABILITY STATEMENT

The data that support the findings of this study are available from the corresponding author upon reasonable request.

ORCID

Rie Sonoi https://orcid.org/0000-0002-8597-8942

REFERENCES

1. Yoshizato K, Tateno C. A human hepatocyte-bearing mouse: an animal model to predict drug metabolism and effectiveness in humans. *PPAR Res*. 2009;2009:476217. doi:10.1155/2009/476217
2. Yoshizato K, Tateno C, Utoh R. Mice with liver composed of human hepatocytes as an animal model for drug testing. *Curr Drug Discov Technol*. 2012;9(1):63-76. doi:10.2174/157016312799304570
3. Andersson TB, Kanebratt KP, Kenna JG. The HepaRG cell line: a unique in vitro tool for understanding drug metabolism and toxicology in human. *Expert Opin Drug Metab Toxicol*. 2012;8(7):909-920. doi:10.1517/17425255.2012.68515
4. Satoh T, Sugiura S, Shin K, et al. A multi-throughput multi-organ-on-a-chip system on a plate formatted pneumatic pressure-driven medium circulation platform. *Lab Chip*. 2017;18(1):115-125. doi:10.1039/c7lc00952f
5. Kojima K, Nakamura H, Komeya M, et al. Neonatal testis growth recreated in vitro by two-dimensional organ spreading. *Biotechnol Bioeng*. 2018;115(12):3030-3041. doi:10.1002/bit.26822
6. Hofer M, Lutolf MP. Engineering organoids. *Nat Rev Mater*. 2021;6(5):402-420. doi:10.1038/s41578-021-00279-y
7. Pedersen JM, Matsson P, Bergström CAS, et al. Early identification of clinically relevant drug interactions with the human bile salt export pump (BSEP/ABCB11). *Toxicol Sci*. 2013;136(2):328-343. doi:10.1093/toxsci/kft197
8. Qiu XI, Zhang Y, Liu T, et al. Disruption of BSEP function in HepaRG cells alters bile acid disposition and is a susceptive factor to drug-induced cholestatic injury. *Mol Pharm*. 2016;13(4):1206-1216. doi:10.1021/acs.molpharmaceut.5b00659
9. Braga VMM, Machesky LM, Hall A, et al. The small GTPases Rho and Rac are required for the establishment of cadherin-dependent cell-cell contacts. *J Cell Biol*. 1997;137(6):1421-1431. doi:10.1083/jcb.137.6.1421
10. Burbank MG, Burban A, Sharanek A, et al. Early alterations of bile canaliculi dynamics and the Rho kinase/myosin light chain kinase pathway are characteristics of drug-induced intrahepatic cholestasis. *Drug Metab Dispos*. 2016;44(11):1780-1793. doi:10.1124/dmd.116.071373
11. Sharanek A, Burban A, Burbank M, et al. Rho-kinase/myosin light chain kinase pathway plays a key role in the impairment of bile canaliculi dynamics induced by cholestatic drugs. *Sci Rep*. 2016;6:24709. doi:10.1038/srep24709
12. Itoh M, Nagafuchi A, Moroi S, et al. Involvement of ZO-1 in cadherin-based cell adhesion through its direct binding to alpha catenin and actin filaments. *J Cell Biol*. 1997;138(1):181-192. doi:10.1083/jcb.138.1.181
13. Fanning AS, Jameson BJ, Jesaitis LA, et al. The tight junction protein ZO-1 establishes a link between the transmembrane protein occludin and the actin cytoskeleton. *J Biol Chem*. 1998;273(45):29745-29753. doi:10.1074/jbc.273.45.29745
14. Sonoi R, Hagihara Y. Tight junction stabilization prevents HepaRG cell death in drug-induced intrahepatic cholestasis. *Biol Open*. 2021;10(6):bio058606. doi:10.1242/bio.058606
15. Fisher A, Croft-Baker J, Davis M, et al. Entacapone-induced hepatotoxicity and hepatic dysfunction. *Mov Disord*. 2002;17(6):1362-1365. doi:10.1002/mds.10342
16. Haasio K. Toxicology and safety of COMT inhibitors. *Int Rev Neurobiol*. 2010;95:163-189. doi:10.1016/B978-0-12-381326-8.00007-7

17. Schneider CA, Rasband WS, Eliceiri KW. NIH image to ImageJ: 25 years of image analysis. *Nat Methods*. 2012;9(7):671-675. doi:10.1038/nmeth.2089
18. Fu D, Wakabayashi Y, Lippincott-Schwartz J, et al. Bile acid stimulates hepatocyte polarization through a cAMP-Epac-MEK-LKB1-AMPK pathway. *Proc Natl Acad Sci USA*. 2011;108(4):1403-1408. doi:10.1073/pnas.1018376108
19. Nguyen A, Bouscarel B. Bile acids and signal transduction: role in glucose homeostasis. *Cell Signal*. 2008;20(12):2180-2197. doi:10.1016/j.cellsig.2008.06.014
20. Mitic LL, Anderson JM. Molecular architecture of tight junctions. *Annu Rev Physiol*. 1998;60:121-142. doi:10.1146/annurev.physiol.60.1.121
21. Citi S. The mechanobiology of tight junctions. *Biophys Rev*. 2019;11(5):783-793. doi:10.1007/s12551-019-00582-7
22. Grünig D, Felser A, Bouitbir J, et al. The catechol-O-methyltransferase inhibitors tolcapone and entacapone uncouple and inhibit the mitochondrial respiratory chain in HepaRG cells. *Toxicol in Vitro*. 2017;42:337-347. doi:10.1016/j.tiv.2017.05.013
23. Grünig D, Felser A, Duthaler U, et al. Effect of the catechol-O-methyltransferase inhibitors tolcapone and entacapone on fatty acid metabolism in HepaRG cells. *Toxicol Sci*. 2018;164(2):477-488. doi:10.1093/toxsci/kfy101
24. Gao S-Y, Li C-Y, Shimokawa T, et al. Rho-family small GTPases are involved in forskolin-induced cell-cell contact formation of renal glomerular podocytes in vitro. *Cell Tissue Res*. 2007;328(2):391-400. doi:10.1007/s00441-006-0365-3
25. Sonoi R, Hagihara Y. Switching of cell fate through the regulation of cell growth during drug-induced intrahepatic cholestasis. *J Biosci Bioeng*. 2020;130(6):659-665. doi:10.1016/j.jbiosc.2020.08.004
26. Lima WR, Parreira KS, Devuyst O, et al. ZONAB promotes proliferation and represses differentiation of proximal tubule epithelial cells. *J Am Soc Nephrol*. 2010;21(3):478-488. doi:10.1681/ASN.2009070698
27. Kampik D, Basche M, Georgiadis A, et al. Modulation of contact inhibition by ZO-1/ZONAB gene transfer-A New strategy to increase the endothelial cell density of corneal grafts. *Invest Ophthalmol Vis Sci*. 2019;60(8):3170-3177. doi:10.1167/iovs.18-26260
28. Balda MS, Matter K. The tight junction protein ZO-1 and an interacting transcription factor regulate ErbB-2 expression. *EMBO J*. 2000;19(9):2024-2033. doi:10.1093/emboj/19.9.2024
29. Balda MS, Garrett MD, Matter K. The ZO-1-associated Y-box factor ZONAB regulates epithelial cell proliferation and cell density. *J Cell Biol*. 2003;160(3):423-432. doi:10.1083/jcb.200210020
30. Schwayer C, Shamipour S, Pranjic-Ferscha K, et al. Mechanosensation of tight junctions depends on ZO-1 phase separation and flow. *Cell*. 2019;179(4):937-952. doi:10.1016/j.cell.2019.10.006
31. Kreft M, Stenovec M, Zorec R. Focus-drift correction in time-lapse confocal imaging. *Ann N Y Acad Sci*. 2005;1048:321-330. doi:10.1196/annals.1342.029
32. Khodjakov A, Rieder CL. Imaging the division process in living tissue culture cells. *Methods*. 2006;38(1):2-16. doi:10.1016/j.ymeth.2005.07.007
33. Peters J. Environmental considerations for live cell imaging. *Nikon Application Notes*. 2008;9:1-4.
34. Xu Y, Wang XU, Zhai C, et al. A single-shot auto focus approach for surface plasmon resonance microscopy. *Anal Chem*. 2021;93(4):2433-2439. doi:10.1021/acs.analchem.0c04377
35. Sonoi R, Kim MH, Kino-oka M. Locational heterogeneity of maturation by changes in migratory behaviors of human retinal pigment epithelial cells in culture. *J Biosci Bioeng*. 2015;119(1):107-112. doi:10.1016/j.jbiosc.2014.05.025
36. Shuzui E, Kim MH, Kino-oka M. Anomalous cell migration triggers a switch to deviation from the undifferentiated state in colonies of human induced pluripotent stems on feeder layers. *J Biosci Bioeng*. 2019;127(2):246-255. doi:10.1016/j.jbiosc.2018.07.020

SUPPORTING INFORMATION

Additional supporting information may be found in the online version of the article at the publisher's website.

How to cite this article: Sonoi R, Hagihara Y. Quantitative understanding of HepaRG cells during drug-induced intrahepatic cholestasis through changes in bile canaliculi dynamics. *Pharmacol Res Perspect*. 2022;10:e00960. doi:10.1002/prp2.960